Point-dipole approximation for surface plasmon polariton scattering: Implications and limitations

A. B. Evlyukhin*
Department of Physics and Applied Mathematics, Vladimir State University, Gorkii str. 87, Vladimir, 600000, Russia

S. I. Bozhevolnyi
Department of Physics and Nanotechnology, Aalborg University, Pontoppidanstræde 103, DK-9220 Aalborg Ø, Denmark
(Received 15 December 2004; published 13 April 2005)

We consider in detail the point-dipole approximation of surface plasmon polariton (SPP) scattering and its limitations imposed by the energy conservation. In the framework of the point-dipole approach, we analytically calculate the scattered electric fields of both the waves propagating away from a metal-dielectric interface and SPP waves. This allows us to establish the relation between the scalar and vectorial models of SPP scattering by dipolar particle. The differential and total scattering cross sections related to SPP-to-SPP scattering and scattering of SPP's into waves propagating away from the interface are studied with respect to the configuration and material parameters of the system. Using the Poynting theorem, we show that the condition of constant field inside a dipolelike scatterer is also essential for the energy conservation in the scattering process, resulting in additional requirements on the sphere radius and other system parameters. In addition to the general case, different limiting cases are considered exemplifying the relative importance of these requirements.

DOI: 10.1103/PhysRevB.71.134304 PACS number(s): 78.68.+m, 71.36.+c, 02.70.−c, 03.65.Nk

I. INTRODUCTION

Surface plasmon polaritons (SPP's) are confined electromagnetic waves that propagate along a dielectric-metal interface with amplitudes that decay exponentially with increasing distance into both of the neighboring media.[1] SPP's exhibit a very high sensitivity to surface properties, e.g., surface roughness and adsorbates. The SPP behavior has been extensively studied, especially the SPP scattering into the far-field zone by surface random roughness.[1] Renewed interest in SPP's comes from recent advances in nanotechnology that allow one to fabricate artificial surface microstructures and nanostructures in order to control and manipulate SPP properties. One of the most attractive aspects of SPP's is the possibility of concentrating and guiding electromagnetic radiation using subwavelength structures.[2] Extensive theoretical and experimental investigations of SPP properties have been carried out during the last ten years. Thus various theoretical simulations of SPP scattering and reflection by surface defects have been reported.[3–7] The SPP propagation along one-dimensional surface structure[8,9] and the coupling between SPP's on a homogeneous thin film and modes sustained by metal stripes[10] have been experimentally investigated. Demonstrations of SPP microcomponents, such as mirrors, beam splitters, etc., made of individual microscatterers have been reported,[11,12] including the realization of an efficient SPP interferometer.[13] Properties of SPP's at terahertz frequencies, that might be interesting for direct and simple biosensing, have been experimentally investigated.[14] Quite recently, periodical microstructures of gold nanoparticles have been shown to exhibit band gap properties for SPP's.[15–17] Furthermore, SPP waveguiding along straight and bent line defects in the periodic structures has also been demonstrated.[17–19] In general, the SPP band-gap (BG) phenomenon[20,21] is similar to the photonic band-gap effect.[22]

However the progress in SPP optics of artificial (and specifically designed) systems of nanoparticles raises new problems that should be solved for the potential of SPP optics to be fully realized. For example, the process of (inelastic) SPP scattering out of the surface plane (into waves propagating away from the surface) should be investigated in detail in order to minimize the inelastic SPP scattering while maximizing the efficiency of the in-plane (elastic) SPP scattering by surface nanostructures. This issue becomes especially important in the case of strong multiple SPP scattering, occurring, for example, in the aforementioned band-gap structures. In general, the task of SPP scattering by surface inhomogeneities is very complicated, and even a relatively simple case of the SPP scattering by a single symmetric defect requires elaborate numerical simulations.[23] The problem becomes even more complicated when one considers sophisticated surface structures consisting of surface nanoparticles as in various optical microcomponents, e.g., line mirrors and beam splitters[24,25] and band-gap structures.[15,16] In order to approach the problem of multiple SPP scattering by a complicated system of scatterers one is forced to seek a compromise between the complexity of a system considered and the accuracy of a model employed. This means that when treating an ensemble of (many) scatterers one usually opts for a (relatively) simple description of SPP scattering by an individual scatterer. A possible approach in such a case is to make use of the point-dipole approximation. In the framework of this approach, the local spectroscopy of noble metal nanoparticle structure deposited on a transparent sample with surface electromagnetic evanescent field has been theoretically analyzed in Ref. 26. The SPP local excitation and scattering (both in and out of the surface plane) by surface particles have been described and simulated in the context of near-

field (forbidden-light) microscopy.[27] In addition, scalar and vectorial models of micro-optical SPP components[24] and band-gap structures[15,16] have been developed. These models allowed one to circumvent a complicated problem of scattering inside surface particles and concentrate the efforts on modeling of (strong multiple) scattering between the particles, simulating various scattering phenomena that were experimentally observed. However, up to now the potential of the point-dipole approximation for SPP scattering has not been fully explored, and the limits of its validity have not been established.

The main purpose of this paper is to consider in detail the point-dipole approximation of SPP scattering and its limitations imposed by the energy conservation. The point-dipole approximation is based on the assumption of constant field inside a scatterer (spherical particle) so that the excitation of higher-order multipole components in the scattering field can be neglected. The usual requirement is that the radius R_p of a spherical particle should be sufficiently small in comparison with both the light wavelength and the distance z_p between the center of the particle and the surface.[28–31] Here, it will be shown that the condition of constant field is also essential for the energy conservation that results in additional requirements on the sphere radius and other system parameters. In order to express the main relations in an analytic form we will have to neglect the material absorption in some cases that will be explicitly indicated. This assumption can be justified by the fact that the SPP propagation length along the plane surface of noble metals is about two orders of magnitude larger than the wavelength of light in visible and even larger in infrared.[2]

The paper is organized as follows. In Sec. II, the main formulas of the SPP scattering by a point dipole are given, and the relation between the scalar and vectorial models is established. In Sec. III, we calculate the differential and total cross sections for the two SPP scattering mechanisms. The results of the preceding sections are used to consider the energy conservation in scattering processes, establishing the conditions that should be fulfilled in Sec. IV. The results are summarized and the conclusions are offered in Sec. V.

II. SPP SCATTERING BY A POINT DIPOLE: MAIN FORMULAE

Let us consider the following physical system (Fig. 1). A small spherical particle with radius R_p and dielectric constant ε_p is located in a reference system, which consists of a dielectric (in the region $z>0$) with dielectric constant $\varepsilon_r>0$ and a metal (in the region $z<0$) with dielectric constant ε_m. The particle is located above the metal surface in the dielectric half space, its position being given by $\mathbf{r}_p=(0,0,z_p)$. The metal-dielectric interface is assumed to support the propagation of SPP's, implying that $\mathrm{Re}(\varepsilon_m)<-\varepsilon_r$. A plane SPP wave (at frequency ω) is propagated along the surface in the x direction, incident on and scattered by the particle (Fig. 1). The incident SPP electric field $\mathbf{E}_0$ field can be represented in the following form:[16,31]

$$\mathbf{E}_0 = \exp(ik_{\mathrm{SPP}}x - ak_{\mathrm{SPP}}z)(-ia\hat{x},0,\hat{z}),\ z>0, \tag{1}$$

where $a=\sqrt{\varepsilon_r/(-\varepsilon_m)}$; $k_{\mathrm{SPP}}=k_0\sqrt{\varepsilon_r\varepsilon_m/(\varepsilon_r+\varepsilon_m)}$ is the SPP wave number; k_0 is the wave number in the vacuum; $\hat{x}$, $\hat{y}$, $\hat{z}$ are the coordinate unit vectors; and $1/(ak_{\mathrm{SPP}})$ and a/k_{SPP} determine the SPP penetration depths in the dielectric and metal, respectively.

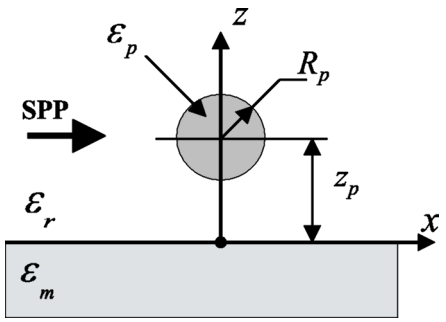

FIG. 1. Schematic representation of physical system: SPP wave is scattered by a spherical particle with radius R_p and dielectric constant ε_p.

In the electric point-dipole approximation,[16,27,32] the particle is treated as a dipolar scatterer located at $\mathbf{r}_p$, and the total electric field everywhere outside the particle can be expressed as

$$\mathbf{E}_{\mathrm{total}}(\mathbf{r}) = \mathbf{E}_0(\mathbf{r}) + \frac{k_0^2}{\varepsilon_0}\hat{G}(\mathbf{r},\mathbf{r}_p)\mathbf{p}, \tag{2}$$

where $\mathbf{E}_0(\mathbf{r})$ is the electric field of the incident SPP wave at point $\mathbf{r}$, ε_0 is the vacuum permittivity, the vector $\mathbf{p}$ denotes the dipole moment of the particle, and $\hat{G}(\mathbf{r},\mathbf{r}')$ is the dyadic Green's function of the reference system, i.e., the physical system without the particle. The second term on the right-hand side of Eq. (2) is the scattered field $\mathbf{E}_{\mathrm{sc}}(\mathbf{r})$. Sometimes it is convenient to split $\hat{G}(\mathbf{r},\mathbf{r}')$ into two separate contributions, viz. the Green's function of the homogeneous medium $\hat{G}^0(\mathbf{r},\mathbf{r}')$ and that related to the reflection from the interface $\hat{G}^s(\mathbf{r},\mathbf{r}')$.[27] However, if one considers scattering processes involving SPP's, it is more convenient to apply another approach that has been recently reported.[31] In this formulation, the Green's tensor is divided into the part that governs the excitation of SPP's, $\hat{G}_{\mathrm{SPP}}(\mathbf{r},\mathbf{r}')$, those describing s- and p-polarized waves that propagate away from the interface, $\hat{G}_T^{s\text{-pol}}(\mathbf{r},\mathbf{r}')$ and $\hat{G}_T^{p\text{-pol}}(\mathbf{r},\mathbf{r}')$, and the quasistatic (near) field contributions $\hat{G}_q^0(\mathbf{r},\mathbf{r}')+\hat{G}_q^s(\mathbf{r},\mathbf{r}')$, corresponding, respectively, to the two aforementioned contributions:

$$\hat{G}(\mathbf{r},\mathbf{r}') = \hat{G}_q^0(\mathbf{r},\mathbf{r}') + \hat{G}_q^s(\mathbf{r},\mathbf{r}') + \hat{G}_T^{s\text{-pol}}(\mathbf{r},\mathbf{r}') + \hat{G}_T^{p\text{-pol}}(\mathbf{r},\mathbf{r}') + \hat{G}_{\mathrm{SPP}}(\mathbf{r},\mathbf{r}'). \tag{3}$$

In order to calculate the scattered field one has to determine the dipole moment of the scatterer as well. The induced dipole moment of a small particle can be expressed as follows:

$$\mathbf{p} = \hat{\alpha}_d\mathbf{E}_0, \tag{4}$$

where $\hat{\alpha}_d$ is the polarizability tensor accounting for the surface dressing effect[16,33]

$$\hat{\alpha}_d = \alpha_0 \left(\hat{\mathbf{I}} - k_0^2 \frac{\alpha_0}{\varepsilon_0} \cdot \hat{G}^s(\mathbf{r}_p, \mathbf{r}_p) \right)^{-1} \tag{5}$$

and $\hat{\mathbf{I}}$ is the unit dyadic tensor. The polarizability of a spherical small particle with the volume $V_p = 4\pi R_p^3/3$ is given by

$$\alpha_0 = \varepsilon_0 \varepsilon_r V_p 3 \frac{\varepsilon_p - \varepsilon_r}{\varepsilon_p + 2\varepsilon_r}. \tag{6}$$

Finally, using the electrostatic approximation of the Green's function $\hat{G}^s(\mathbf{r}, \mathbf{r}')$,[32,34–36] we obtain

$$\hat{\alpha}_d = \alpha_0 \left(\frac{1}{1 + \xi\beta} \hat{x}\hat{x} + \frac{1}{1 + \xi\beta} \hat{y}\hat{y} + \frac{1}{1 + 2\xi\beta} \hat{z}\hat{z} \right), \tag{7}$$

where we introduced two parameters of the surface dressing effect, viz. a geometrical parameter $\beta = [R_p/(2z_p)]^3$ and a material one $\xi = [(\varepsilon_r - \varepsilon_m)(\varepsilon_p - \varepsilon_r)]/[(\varepsilon_r + \varepsilon_m)(\varepsilon_p + 2\varepsilon_r)]$. These parameters reflect the fact that the dressing effect can be equally influenced by adjusting the system geometry and dielectric susceptibilities involved.

In general, the calculation of different contributions in the scattering field involves numerical integrations of the Sommerfeld-type integrals.[27,31] The procedure is rather time consuming especially with many combinations of observation points and source points being considered. However, if one considers fractions of the scattered field that correspond to SPP waves and electromagnetic waves propagating away from the interface, i.e., to the scattered far-field components, one can replace the Green's tensor of the reference system by its far-field approximation. Relatively simple analytical representations for $\hat{G}_{\mathrm{SPP}}(\mathbf{r}, \mathbf{r}')$ and $\hat{G}_T^{s\text{-pol}}(\mathbf{r}, \mathbf{r}') + \hat{G}_T^{p\text{-pol}}(\mathbf{r}, \mathbf{r}')$ have been obtained in Refs. 31 and 37, respectively. These representations are especially useful when dealing with arrays of scatterers, e.g., forming a periodic lattice exhibiting the band-gap effect for SPPs.[16,25]

A. Scattered SPP waves

In the case where the distance along the interface between a source and an observation point is large, with both points being close to the surface plane (in comparison with the light wavelength in both cases), an analytical approximation of $\hat{G}_{\mathrm{SPP}}(\mathbf{r}, \mathbf{r}')$ can be written down in the cylindrical coordinates[31]

$$\hat{G}_{\mathrm{SPP}}(\mathbf{r}, \mathbf{r}') = \frac{iak_{\mathrm{SPP}} H_0^{(1)}(k_{\mathrm{SPP}}\rho) e^{-ak_{\mathrm{SPP}}(z+z')}}{2(1-a^4)(1-a^2)} \times [\hat{z}\hat{z} + a^2 \hat{\rho}\hat{\rho} + (\hat{z}\hat{\rho} - \hat{\rho}\hat{z})ia], \tag{8}$$

where $\mathbf{r} = (x, y, z)$ points to the observation point in the upper half-space $z > 0$, $\mathbf{r}' = (0, 0, z')$ points to the source of scattering, $\hat{\rho} = \boldsymbol{\rho}/\rho$ [$\boldsymbol{\rho} = (x, y)$, $\rho = |\boldsymbol{\rho}|$], and $H_0^{(1)}$ is the zero-order Hankel function of the first kind. The approximation (8) was found very useful for evaluating multiple scattering between particles located close to a metal surface and modeling of the corresponding SPP scattering phenomena.[16,25] Thus, it has been used for simulations of finite SPP band-gap structures and the SPP waveguiding along channels in these structures,[16] replicating main features of the experimentally observed phenomena.[17]

It is interesting to note that successful (to a certain extent) attempts to simulate SPP scattering by various configurations of surface scatterers including band-gap structures have been carried out in the framework of a scalar approximation.[15,24] In this approximation, the SPP-to-SPP scattering by a small particle located near the metal-dielectric interface is described with the following relation:

$$E_{\mathrm{sc}}(\mathbf{r}) = \alpha_e E_0(\mathbf{r}_p) G(\mathbf{r}, \mathbf{r}_p), \tag{9}$$

where $G(\mathbf{r}, \mathbf{r}_p) = iH_0^{(1)}(k_{\mathrm{SPP}}\rho)/4$, E_0 and E_{sc} are the electric z components of the incident and scattered SPP fields at the metal surface, and α_e is the effective polarizability of a scatterer located at $\mathbf{r}_p$. Note that, in this model, the SPP scattering by an individual dipolelike particle is isotropic.

In order to relate the vectorial and scalar models of the SPP-to-SPP scattering let us write down the z component of the scattered SPP electric field in the framework of the vectorial approach by making use of Eqs. (4) and (8):

$$E_z(\rho, \varphi, z) = AH_0^{(1)}(k_{\mathrm{SPP}}\rho) \frac{\alpha_0}{1 + 2\xi\beta} \times (1 + \eta_p \cos\varphi) e^{-ak_{\mathrm{SPP}}(z + 2z_p)}, \tag{10}$$

where ρ and φ are cylindrical in-plane coordinates,

$$A = \frac{iak_0^2 k_{\mathrm{SPP}}}{2\varepsilon_0 (1 - a^4)(1 - a^2)}, \tag{11}$$

$$\eta_p = \frac{a^2(1 + 2\xi\beta)}{1 + \xi\beta}. \tag{12}$$

Note that the other nonzero SPP field component is $E_\rho = -iaE_z$. Comparison of the SPP field z components used in the two models [cf. Eqs. (9) and (10)] shows that the vectorial approach reduces to the scalar one, if the inequality $|a| \ll 1$ is satisfied. Indeed, in this case, the (transverse) z component of the SPP electric field becomes much larger than the longitudinal one, and the SPP part of the Green's tensor reduces to a scalar function. As a result, one can consider the SPP-to-SPP scattering with reasonable accuracy by using the scalar model. For example, in the scalar model of finite-size SPP band-gap structures,[15] this parameter was $|a| \approx 0.2$, and the simulations were found in qualitative agreement with the experimental results.

The vectorial model[31] allows one, however, not only to accurately take into account all components of SPP fields but also to correctly introduce the polarizability of a scatterer, as well as to analytically evaluate the effective polarizability α_e used in the scalar model. The latter can be conveniently expressed under the condition of $|a| \ll 1$ as follows:

$$\alpha_e \simeq \frac{6ak_0^3 \varepsilon_r^{3/2} V_p (\varepsilon_p - \varepsilon_r)}{(\varepsilon_p + 2\varepsilon_r - 2(\varepsilon_p - \varepsilon_r)\beta)}. \tag{13}$$

It is interesting to estimate, with the help of Eq. (13), the size of a scatterer that would correspond to the effective polarizability used in Ref. 24, in which the scalar model for the SPP scattering was first introduced. Using the appropriate param-

eter values $\alpha_e=3$, light wavelength $\lambda=633$ nm, $\varepsilon_m=\varepsilon_p=-16+i$, $\varepsilon_r=1$,[24] and assuming that $R_p=z_p$, we obtain the scatterer radius $R_p\approx 70$ nm. This value seems reasonable[24] and sufficiently small (with respect to the wavelength), so that the point-dipole approach can be considered adequate for the modeling of SPP scattering phenomena.

B. Scattered *s*- and *p*-polarized waves

Scattered *s*- and *p*-polarized waves propagating away from the surface into medium with ε_r are composed of the waves directly scattered by a particle and those reflected by the surface. Using the results obtained by Novotny[37] for the layered structures and transforming it for a one-interface system, we obtain the following expressions (in the spherical coordinates) for the components of the scattered electric field:

$$E_\varphi = \frac{i}{a}\frac{k_0^2}{\varepsilon_0}\frac{\alpha_0}{1+2\xi\beta}\eta_p \sin\varphi(1+r^{(s)}e^{ik_r 2z_p\cos\theta}) \times \frac{e^{ik_r r}}{4\pi r}e^{-ak_{\mathrm{SPP}}z_p - ik_r z_p\cos\theta}, \tag{14}$$

$$E_\theta = -\frac{k_0^2}{\varepsilon_0}\frac{\alpha_0}{1+2\xi\beta}\left\{\frac{i}{a}\eta_p\cos\varphi\cos\theta(1-r^{(p)}e^{ik_r 2z_p\cos\theta}) + \sin\theta(1+r^{(p)}e^{ik_r 2z_p\cos\theta})\right\}\frac{e^{ik_r r}}{4\pi r}e^{-ak_{\mathrm{SPP}}z_p - ik_r z_p\cos\theta}, \tag{15}$$

where r is the distance to the observation point, $k_r=k_0\sqrt{\varepsilon_r}$, φ and θ are the azimuthal and polar angles of the spherical coordinate system, respectively, the reflection coefficients $r^{(p)}$ and $r^{(s)}$ for *p*- and *s*-polarized waves are given by

$$r^{(p)} = \frac{\varepsilon_m\cos\theta - \varepsilon_r i\sqrt{\sin^2\theta - \varepsilon_m/\varepsilon_r}}{\varepsilon_m\cos\theta + \varepsilon_r i\sqrt{\sin^2\theta - \varepsilon_m/\varepsilon_r}}, \tag{16}$$

$$r^{(s)} = \frac{\cos\theta - i\sqrt{\sin^2\theta - \varepsilon_m/\varepsilon_r}}{\cos\theta + i\sqrt{\sin^2\theta - \varepsilon_m/\varepsilon_r}}. \tag{17}$$

Although in the next part of this paper we will restrict our consideration to the case of real dielectric constants, the above expressions for the fields can be also used in the case of metals with complex dielectric constants.[31]

III. SCATTERING CROSS-SECTIONS

In order to compare the efficiency of the SPP-to-SPP scattering with that of the SPP scattering into the waves propagating away from the metal surface, let us calculate the differential and total cross sections for the both scattering channels. In the following, only the case of real dielectric constants will be considered.

A. SPP-to-SPP scattering

The differential cross section of the SPP-to-SPP scattering can be determined by relating the time-averaged Poynting vectors of incident and scattered SPP waves:[23]

$$\sigma_{\mathrm{SPP}}(\varphi)d\varphi = \frac{\int_{-\infty}^{\infty}\langle \mathbf{S}_{\mathrm{SPP}}\rangle_\rho dz\rho d\varphi}{\int_{y_1}^{y_2}\int_{-\infty}^{\infty}\langle \mathbf{S}_{\mathrm{in}}\rangle dydz/(y_2-y_1)}, \tag{18}$$

where the nominator integral expresses the power scattered into the SPP wave in the direction defined by the angle φ, and the denominator integral

$$P_{\mathrm{in}} = \int_{y_1}^{y_2}\int_{-\infty}^{\infty}\langle \mathbf{S}_{\mathrm{in}}\rangle dydz/(y_2-y_1) = \frac{1}{2k_0}\sqrt{\frac{\varepsilon_0}{\mu_0}}\frac{1-a^2}{2a}(1-a^4) \tag{19}$$

is the incident SPP power per unit length. Here μ_0 is the vacuum permeability. Note that the term a^4 in the brackets of Eq. (19) stems from the energy flux below the surface, i.e., in the metal. Therefore, if $a^4=(\varepsilon_r/\varepsilon_m)^2\ll 1$ we can neglect the SPP power concentrated in the metal and restrict the consideration of SPP scattering to the dielectric half-space.

Using the results of the preceding section and the far-field approximation of the Hankel function, one can obtain the following expression for the (only) nonzero component of the time-averaged Poynting vector associated with the scattered SPP wave:

$$\langle \mathbf{S}_{\mathrm{SPP}}\rangle_\rho = \frac{1}{k_0}\sqrt{\frac{\varepsilon_0}{\mu_0}}|A|^2\left(\frac{\alpha_0}{1+2\xi\beta}\right)^2 e^{-2ak_{\mathrm{SPP}}(z+2z_p)} \times \frac{(1+\eta_p\cos\varphi)^2(1-a^2)}{\pi\rho}, \quad z>0. \tag{20}$$

Combining the above relations and carrying the integration out, results in the explicit expression for the differential cross section

$$\sigma_{\mathrm{SPP}}(\varphi) = \frac{2|A|^2(1+\eta_p\cos\varphi)^2}{\pi k_{\mathrm{SPP}}}\left(\frac{\alpha_0}{1+2\xi\beta}\right)^2 e^{-4ak_{\mathrm{SPP}}z_p}. \tag{21}$$

The angular dependence of the scattering cross section is given by $(1+\eta_p\cos\varphi)^2$, with the SPP incident direction corresponding to $\varphi=0$ and η_p being determined by the geometry and material parameters of the surface dressing [Eq. (12)]. Typical dependencies are shown in Fig. 2 for a gold[38] spherical particle located close to the gold surface at different distances with the incident SPP being excited at the light wavelength of 800 nm. It is seen that the SPP-to-SPP scattering (by a small sphere) is in fact anisotropic with the most efficient scattering occurring in the forward direction ($\varphi=0$). Note that the anisotropy is more pronounced for smaller particle-surface distances and, in general, for stronger surface dressing. When comparing the above cross section σ_{SPP} with that obtained in Ref. 23 for a finite-size indentation, it is seen that both exhibit similar size ($\sigma_{\mathrm{SPP}}\sim R_p^6$) and wave number ($\sigma_{\mathrm{SPP}}\sim k_0^5$) dependencies with the scattering being closer to isotropic for smaller scatterers.

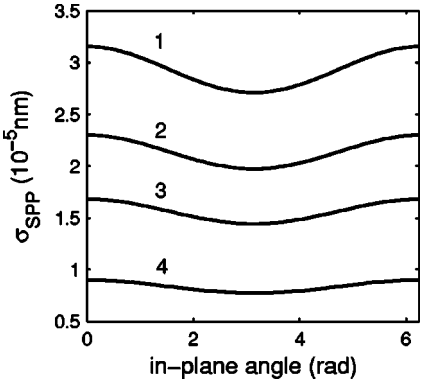

FIG. 2. The differential SPP-to-SPP scattering cross section as a function of the in-plane angle φ for a spherical gold particle with the radius $R_p=10$ nm located near the gold surface at different distances: $z_p=$(1) 50, (2) 100, (3) 150, and (4) 250 nm. Other system parameters are the light wavelength $\lambda=800$ nm and the dielectric constants of air $\varepsilon_r=1$ and gold $\varepsilon_m=\varepsilon_p\approx-26.3$ (Ref. 38).

The total cross section for the SPP-to-SPP scattering is finally obtained by angular integration of the differential cross section given by Eq. (21), resulting in

$$\sigma_{\text{scat}}^{\text{SPP}}=\frac{a^2k_0^4k_{\text{SPP}}(2+\eta_p^2)}{2\varepsilon_0^2(1-a^4)^2(1-a^2)^2}\left(\frac{\alpha_0}{1+2\xi\beta}\right)^2 e^{-4ak_{\text{SPP}}z_p}. \quad (22)$$

It should be mentioned that the SPP-to-SPP scattering cross section is exponentially decreasing with the increase of the particle-surface distance in accord with the SPP penetration depth in dielectric as one would have expected.

B. SPP scattering away from the surface

The flux of radiation into the medium above the surface corresponds to the time-averaged Poynting vector $\langle \mathbf{S}_{\text{space}}\rangle$ that, in the far field, can be expressed in terms of $\mathbf{E}_{\text{sc}}$:

$$\sigma_{\text{space}}(\varphi,\theta)=\frac{\langle \mathbf{S}_{\text{space}}\rangle r^2}{P_{\text{in}}}=\frac{2k_ra}{(1-a^2)(1-a^4)}|\mathbf{E}_{sc}|^2r^2, \quad (23)$$

where $\mathbf{E}_{\text{sc}}$ is determined by Eqs. (14) and (15).

The angular distribution of SPP scattering into the dielectric half-space is strongly dependent upon the particle-surface distance (Fig. 3). When this distance is relatively small [Figs. 3(a) and 3(b)] the particle scatters better in the forward direction ($\varphi=0$). At the same time, the polar angle θ dependence indicates that the scattering is most efficient at oblique angles. With the increase of the particle-surface distance, the scattering in the backward direction ($\varphi=\pi$) becomes more appreciable and the polar angle dependence, more complicated [Figs. 3(c) and 3(d)]. Note that the angular characteristics of scattering by an individual surface defect calculated in Ref. 23 are rather similar to those shown in Fig. 3(a).

The total cross sections for the SPP scattering into the waves propagating away from the surface for the two polarizations are given, respectively, by

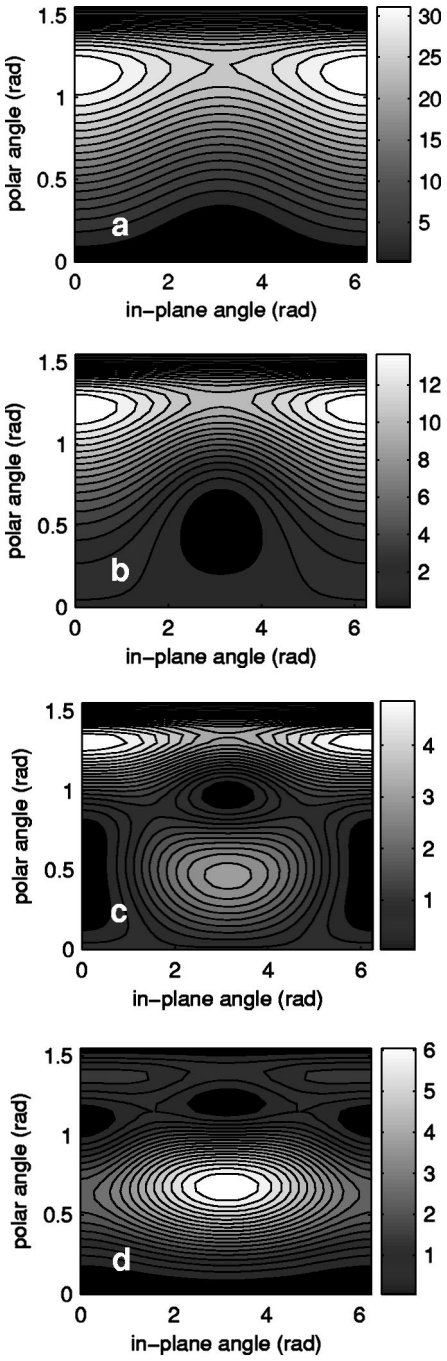

FIG. 3. Differential cross section $\sigma_{\text{space}}(\varphi,\theta)$ ($\times10^{-6}$ nm) for the SPP scattering into the waves propagating away from the gold surface as a function of the in-plane (φ) and polar (θ) angles for a gold spherical particle located near the surface at different distances $z_p=(a)$ 50, (b) 150, (c) 250, and (d) 350 nm. Other system parameters are as in Fig. 2.

$$\sigma_{\text{scat}}^{[s(p)\text{-pol}]}=\int_0^{2\pi}\int_0^{\pi/2}\frac{2k_ra|E_{\varphi(\theta)}(r,\varphi,\theta)|^2}{(1-a^2)(1-a^4)}r^2\sin\theta d\varphi d\theta. \quad (24)$$

Let us now consider the total cross section that includes all channels of scattering into far-field components

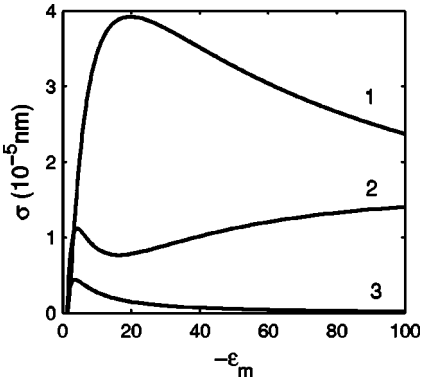

FIG. 4. The total cross sections (1) $\sigma_{\text{scat}}^{\text{SPP}}$, (2) $\sigma_{\text{scat}}^{(p\text{-pol})}$, and (3) $\sigma_{\text{scat}}^{(s\text{-pol})}$ as functions of the bulk dielectric constant ε_m for a gold spherical particle located near the metal surface at the distance $z_p = 300$ nm. Other system parameters are as in Fig. 2.

$$\sigma_{\text{scat}}^{\text{total}} = \sigma_{\text{scat}}^{\text{SPP}} + \sigma_{\text{scat}}^{(s\text{-pol})} + \sigma_{\text{scat}}^{(p\text{-pol})}. \tag{25}$$

Total cross sections for different scattering channels (for a particular scattering configuration) are shown in Fig. 4 as functions of the bulk dielectric constant. It is seen that the SPP-to-SPP scattering can be significantly more efficient than the SPP scattering into the waves propagating away from the metal surface. In general, however, the relative efficiency of SPP-to-SPP scattering decreases with the increase of $|\varepsilon_m|$. Similar tendencies have been noted also for the behavior of the normalized extinction cross section.[31] In the next section, we will determine conditions for the total scattering cross section to be exactly equal to the total extinction cross section within the framework of the point-dipole approximation, establishing thereby limits for its validity.

IV. SPP SCATTERING AND EXTINCTION

Let us apply the integral Poynting's theorem for our case of the SPP scattering by a small spherical particle. After averaging in time one obtains the equation

$$\frac{1}{2}\,\text{Re}\left\{\int_\Sigma [\mathbf{E}_0(\mathbf{r}) \times \mathbf{H}_{\text{sc}}^*(\mathbf{r})]d\mathbf{s} + \int_\Sigma [\mathbf{E}_{\text{sc}}(\mathbf{r}) \times \mathbf{H}_0^*(\mathbf{r})]d\mathbf{s} + \int_\Sigma [\mathbf{E}_{\text{sc}}(\mathbf{r}) \times \mathbf{H}_{\text{sc}}^*(\mathbf{r})]d\mathbf{s}\right\} = 0, \tag{26}$$

where Σ is a closed surface surrounding the scatterer. Here the total electric and magnetic fields are represented as sums of the incident and scattered fields, i.e., $\mathbf{E}_{\text{total}} = \mathbf{E}_0 + \mathbf{E}_{sc}$ and $\mathbf{H}_{\text{total}} = \mathbf{H}_0 + \mathbf{H}_{\text{sc}}$. The expression (26) reflects the fact that the (time-averaged) energy should be conserved in the scattering process. The sum of the first two integrals of the left-hand side of Eq. (26) determines the extinction cross section, whereas the last integral corresponds to the scattering cross section. In the absence of absorption, the extinction and scattering cross sections should be equivalent.[39] We shall use this requirement to establish the validity domain of the point-dipole approximation. Neglecting the SPP scattering into the metal results in

$$\frac{1}{2P_{\text{in}}}\,\text{Re}\left\{\int_\Sigma [\mathbf{E}_{\text{sc}}(\mathbf{r}) \times \mathbf{H}_{\text{sc}}^*(\mathbf{r})]d\mathbf{s}\right\} = \sigma_{\text{scat}}^{\text{total}}, \tag{27}$$

where the incident power P_{in} is given by Eq. (19), and the total scattering cross section $\sigma_{\text{scat}}^{\text{total}}$ is the sum of the cross sections corresponding to the three different scattering channels [Eq. (25)].

The first two terms in Eq. (26) are related to the interference and can be evaluated using the divergence theorem[40] and considering the scattered field produced by a point-dipole scatterer having the dipole moment $\mathbf{p} = \varepsilon_0(\varepsilon_p - \varepsilon_r)V_p\mathbf{E}_{\text{total}}(\mathbf{r}_p)$. After some tedious but straightforward transformations one obtains

$$\frac{1}{2}\,\text{Re}\left\{\int_\Sigma [\mathbf{E}_0(\mathbf{r}) \times \mathbf{H}_{\text{sc}}^*(\mathbf{r})]d\mathbf{s} + \int_\Sigma [\mathbf{E}_{\text{sc}}(\mathbf{r}) \times \mathbf{H}_0^*(\mathbf{r})]d\mathbf{s}\right\} = -\frac{\omega\varepsilon_0(\varepsilon_p - \varepsilon_r)V_p}{2}\,\text{Im}[\mathbf{E}_0^*(\mathbf{r}_p)\mathbf{E}_{\text{total}}(\mathbf{r}_p)]. \tag{28}$$

Note that the left-hand side of Eq. (28) being equal to $-P_{\text{in}}\sigma_{\text{ext}}$ (σ_{ext} is the total extinction cross section) is frequently used in considerations of the extinction, i.e., scattering and absorption, of an isolated scatterer.[39,41,42] Thus, in order to calculate the extinction cross section we should determine the total (self-consistent) field $\mathbf{E}_{\text{total}}(\mathbf{r})$ inside the scatterer.

In order to find the total field inside the particle let us make use of the Lippmann-Schwinger equation

$$\mathbf{E}_{\text{total}}(\mathbf{r}) = \mathbf{E}_0(\mathbf{r}) + k_0^2\int_{V_p} \hat{G}(\mathbf{r},\mathbf{r}')(\varepsilon_p - \varepsilon_r)\mathbf{E}_{\text{total}}(\mathbf{r}')d\mathbf{r}', \tag{29}$$

where $\hat{G}(\mathbf{r},\mathbf{r}')$ is the dyadic Green's function of the reference system. Note that in the framework of the point-dipole approximation, the field inside a scatterer is considered to be constant. It is further convenient to decompose the Green's function into the separate contributions [Eq. (3)] whose integrals should be evaluated. Using the result for a spherical particle

$$\int_{V_p} \hat{G}_q^0(\mathbf{r}_p,\mathbf{r})d\mathbf{r} = -\frac{1}{3k_0^2\varepsilon_r}\hat{\mathbf{I}} \tag{30}$$

and the approximation ($R \ll z_p$)

$$\int_{V_p} \hat{G}_q^s(\mathbf{r}_p,\mathbf{r})d\mathbf{r} \simeq V_p\hat{G}_q^s(\mathbf{r}_p,\mathbf{r}_p), \tag{31}$$

one obtains from Eq. (29)

$$\mathbf{E}_{\text{total}}(\mathbf{r}_p) \approx \frac{3\varepsilon_r}{\varepsilon_p + 2\varepsilon_r}\left[\hat{\mathbf{I}} - \frac{k_0^2}{\varepsilon_0}\alpha_0\hat{G}_q^s(\mathbf{r}_p,\mathbf{r}_p)\right]^{-1}\left(\hat{\mathbf{I}} + \frac{k_0^2}{\varepsilon_0 V_p}\alpha_0 \times\left[\hat{\mathbf{I}} - \frac{k_0^2}{\varepsilon_0}\alpha_0\hat{G}_q^s(\mathbf{r}_p,\mathbf{r}_p)\right]^{-1} \times \int_{V_p} [\hat{G}_T^{s\text{-pol}}(\mathbf{r}_p,\mathbf{r}) + \hat{G}_T^{p\text{-pol}}(\mathbf{r}_p,\mathbf{r}) + \hat{G}_{\text{SPP}}(\mathbf{r}_p,\mathbf{r})]d\mathbf{r}\right)\mathbf{E}_0(\mathbf{r}_p). \tag{32}$$

Here the contribution of the transverse and SPP wave components is assumed to be small in comparison with the quasistatic one. The conditions for the validity of this assumption will be formulated below. Note that if we considered only the qusistatic contribution, the interference term would have been equal to zero (the quasistatic field do not carry the energy away from the scatterer).

Inserting Eq. (32) in the right-hand side of Eq. (28) and taking into account that imaginary parts of the transverse and SPP contributions to the Green's function are nonsingular and can be therefore considered constant inside a small particle, one obtains

$$P_{\text{in}}\sigma_{\text{ext}} = \frac{\omega k_0^2}{2\varepsilon_0}\hat{\alpha}_d\hat{\alpha}_d\mathbf{E}_0^*(\mathbf{r}_p)\text{Im}\{\hat{G}_T^{s\text{-pol}}(\mathbf{r}_p,\mathbf{r}_p) + \hat{G}_T^{p\text{-pol}}(\mathbf{r}_p,\mathbf{r}_p) + \hat{G}_{\text{SPP}}(\mathbf{r}_p,\mathbf{r}_p)\}\mathbf{E}_0(\mathbf{r}_p). \quad (33)$$

The imaginary parts of the tensors $\hat{G}_T^{s\text{-pol}}(\mathbf{r}_p,\mathbf{r}_p) + \hat{G}_T^{p\text{-pol}}(\mathbf{r}_p,\mathbf{r}_p)$ and $\hat{G}_{\text{SPP}}(\mathbf{r}_p,\mathbf{r}_p)$ have been calculated in Ref. 31. The total extinction cross section can be represented as the sum of different parts corresponding to the SPP scattering into *s*-polarized and *p*-polarized waves propagating away from the surface and SPP's:

$$\sigma_{\text{ext}} = \sigma_{\text{ext}}^{(s\text{-pol})} + \sigma_{\text{ext}}^{(p\text{-pol})} + \sigma_{\text{ext}}^{\text{SPP}}. \quad (34)$$

In the absence of absorption, the following relation should be valid [Eq. (26)]:

$$\sigma_{\text{scat}}^{s\text{-pol}} + \sigma_{\text{scat}}^{p\text{-pol}} + \sigma_{\text{scat}}^{\text{SPP}} = \sigma_{\text{ext}}^{s\text{-pol}} + \sigma_{\text{ext}}^{p\text{-pol}} + \sigma_{\text{ext}}^{\text{SPP}}. \quad (35)$$

Comparison of the expressions for the extinction cross sections[31] with those for the scattering cross sections [Eqs. (22) and (24)] shows that this is indeed the case, validating thereby the energy conservation in the considered scattering process.

In this context the main additional assumption used is related to the possibility of neglecting the contributions of the transverse and SPP scattered fields in comparison with that of the quasistatic field inside the scatterer. The corresponding requirements can be obtained from Eq. (32) and the explicit expressions for the transverse Green's tensor of homogeneous medium[43] with ε_r in the limit $R_p k_r \ll 1$ and for the SPP part of the metal-dielectric interface Green's function.[31] There are two conditions related to the SPP field:

$$\left|1 - \frac{(1+a^2)(\varepsilon_p-\varepsilon_r)}{8(1-a^2)(\varepsilon_p+2\varepsilon_r)}\left(\frac{R_p}{z_p}\right)^3\right| \gg \frac{3}{2}k_0^3 V_p\left|\frac{\varepsilon_p-\varepsilon_r}{\varepsilon_p+2\varepsilon_r}\right|\frac{a^3\varepsilon_r^{3/2}F(ak_{\text{SPP}}z_p)}{(1-a^2)^{3/2}(1-a^4)}, \quad (36)$$

$$\left|1 - \frac{(1+a^2)(\varepsilon_p-\varepsilon_r)}{4(1-a^2)(\varepsilon_p+2\varepsilon_r)}\left(\frac{R_p}{z_p}\right)^3\right| \gg 3k_0^3 V_p\left|\frac{\varepsilon_p-\varepsilon_r}{\varepsilon_p+2\varepsilon_r}\right|\frac{a\varepsilon_r^{3/2}F(ak_{\text{SPP}}z_p)}{(1-a^2)^{3/2}(1-a^4)}, \quad (37)$$

and two conditions for the fields propagating away from the surface

$$\left|1 - \frac{(1+a^2)(\varepsilon_p-\varepsilon_r)R_p^3}{8(1-a^2)(\varepsilon_p+2\varepsilon_r)z_p^3}\right| \gg (k_r R_p)^2\left|\frac{\varepsilon_p-\varepsilon_r}{\varepsilon_p+2\varepsilon_r}\right|, \quad (38)$$

$$\left|1 - \frac{(1+a^2)(\varepsilon_p-\varepsilon_r)R_p^3}{4(1-a^2)(\varepsilon_p+2\varepsilon_r)z_p^3}\right| \gg (k_r R_p)^2\left|\frac{\varepsilon_p-\varepsilon_r}{\varepsilon_p+2\varepsilon_r}\right|. \quad (39)$$

Here we introduced [Eqs. (36) and (37)] the function $F(ak_{\text{SPP}}z_p)$ determined as follows:

$$F = m\left|P\int_0^\infty \frac{x^2 e^{-xak_{\text{SPP}}2z_p}dx}{\pi(1-x^2)}\right| + n\frac{e^{-ak_{\text{SPP}}2z_p}}{2}, \quad (40)$$

where the principal value integral and second term stem from the real and imaginary parts of $\hat{G}_{\text{SPP}}(\mathbf{r}_p,\mathbf{r}_p)$, respectively, and $m=1$ and $n=0$ for the magnitude of the principal value integral being equal to or greater than $0.5\exp(-ak_{\text{SPP}}2z_p)$ and $m=0$ and $n=1$ otherwise. For the estimations, it is convenient to use the following simple approximation:

$$F \simeq \begin{cases} 1/[2\pi z_p a k_{\text{SPP}}], & z_p a k_{\text{SPP}} < 1, \\ 1/[4\pi(z_p a k_{\text{SPP}})^3], & z_p a k_{\text{SPP}} \gg 1. \end{cases} \quad (41)$$

Note that $1/(ak_{\text{SPP}})$ gives the SPP penetration depth in the dielectric.

Another (conventional) assumption is that the quasistatic electric field can be considered constant inside the scatterer. This leads to the following requirements: $R_p \ll 1/k_{\text{SPP}}$ and $R_p \ll z_p$, where the first inequality allows one to neglect variations of the incident field inside the scatterer and the second one ensures that the role of higher-order multipoles appearing due to the proximity of the metal-dielectric interface is negligibly small.[31] It is seen that the inequalities expressed by Eqs. (36)–(39) represent indeed the additional requirements for the point-dipole approximation (in the particular case of the SPP scattering). Finally, it should be noted that the above consideration cannot be applied under the conditions of the so-called configuration resonances,[32] since in this case the series expansion used to obtain Eq. (32) is no longer valid. The conditions expressed in Eqs. (36)–(39) can be simplified in several practical cases.

A. Noble metal-air interface

For vast majority of experiments,[8–19,24] scatterers are made of the same noble metal as the bulk with the dielectric medium being air: $|\varepsilon_m| = |\varepsilon_p| \gg \varepsilon_r = 1$. The two conditions

$$R_p \ll \frac{1}{k_0}, \quad (42)$$

$$\frac{1}{4}\left(\frac{R_p}{z_p}\right)^3 \ll 1, \quad (43)$$

then replace $R_p \ll 1/k_{\text{SPP}}$ and $R_p \ll z_p$, respectively (note that, in this case, $k_{\text{SPP}} \simeq k_0$). Since, at the same time, the scatterers are relatively small and placed on the metal surface, one can safely use the inequality $z_p \ll \lambda$, that in turn means that $z_p a k_0 \leqslant 1$. In such a case, the conditions expressed by Eqs. (36)–(39) become superfluous. Moreover, if $z_p k_0 \ll 1$ then the

TABLE I. The conditions for the point-dipole approach (the light wavelength is equal to 800 nm).

Metal	$\mathrm{Re}(\varepsilon_m)$, $\mathrm{Re}(\varepsilon_p)$	$R_p \ll 1/k_{\mathrm{SPP}}$	Eq. (45)	Eq. (46), $z_p = 50$ nm	Eq. (46), $z_p = 200$ nm	Eq. (47)
Gold	−26.3	$R_p \ll 125$ nm	$R_p \ll 1.487 z_p$	$R_p \ll 71$ nm	$R_p \ll 132$ nm	$R_p \ll 120$ nm
Silver	−28	$R_p \ll 126$ nm	$R_p \ll 1.493 z_p$	$R_p \ll 71$ nm	$R_p \ll 131$ nm	$R_p \ll 120$ nm

condition of Eq. (43) is dominant. And vice versa, if $z_p k_0 \geqslant 1$ then the condition of Eq. (42) is sufficient.

For relatively large particle-surface distances, so that $z_p a k_0 \gg 1$ then the conditions in Eqs. (36) and (37) are reduced to

$$|\varepsilon_m| \left(\frac{R_p}{z_p} \right)^3 \ll 1. \tag{44}$$

This requirement is stronger than that of Eq. (43) and the conditions of Eqs. (42) and (44) should be applied (the former when $z_p > |\varepsilon_m|^{1/3}/k_0$ and the latter otherwise).

B. Weak surface dressing

The SPP propagation length becomes larger when the imaginary part of a metal dielectric constant becomes smaller. For this reason, it is often chosen to operate in the wavelength range being away from the SPP resonant frequency. In this range, surface dressing effects are weak, and one can assume that

$$\left| \frac{(1+a^2)(\varepsilon_p - \varepsilon_r)}{4(1-a^2)(\varepsilon_p + 2\varepsilon_r)} \left(\frac{R_p}{z_p} \right)^3 \right| \ll 1. \tag{45}$$

The conditions of Eqs. (36)–(39) can then be reduced resulting in the following (for the SPP field):

$$3k_0^3 V_p \left| \frac{\varepsilon_p - \varepsilon_r}{\varepsilon_p + 2\varepsilon_r} \right| \frac{a \varepsilon_r^{3/2} F(a k_{\mathrm{SPP}} z_p)}{(1-a^2)^{3/2}(1-a^4)} \ll 1 \tag{46}$$

and, for the fields propagating away from the interface,

$$(k_r R_p)^2 \left| \frac{\varepsilon_p - \varepsilon_r}{\varepsilon_p + 2\varepsilon_r} \right| \ll 1. \tag{47}$$

Thus, in the case of weak surface dressing [Eq. (45)], the point-dipole approach can be used if the conditions expressed by Eqs. (46) and (47), along with $R_p \ll 1/k_{\mathrm{SPP}}$ are satisfied. Numerical evaluations of the radius R_p of a gold (silver)[38] particle placed in vacuum above a gold (silver) substrate, which would satisfy the above requirements imposed by the point-dipole approximation, are presented in Table I.

It is seen that the requirements of Eqs. (45) and (46) are dominant for small values of the particle-surface distances z_p. For relatively large z_p, the condition of Eq. (47) becomes dominant. One notices also that (at least for these system parameters) the condition of weak surface dressing [Eq. (45)] and $R_p \ll 1/k_{\mathrm{SPP}}$ are sufficient for the validity of the point-dipole approximation. At the same time, the strong particle-surface interaction (strong surface dressing) would inevitably result in a strongly inhomogeneous total field that would, in turn, increase the contribution of higher-order multipoles in the scattering process.

V. CONCLUSION

In conclusion, we have considered the SPP scattering by a dipolelike spherical particle located near a metal-dielectric interface, focusing on the differential cross sections for different scattering channels and limitations of the point-dipole approximation. The main formulas of the vectorial and scalar SPP scattering models have been reviewed and compared. It has been shown that the two models become very close in the limit of large magnitude of the real part of metal dielectric constant, and the corresponding relation between the main parameters of scalar and vectorial models has been established. We have further shown that the differential cross section for the SPP-to-SPP scattering is anisotropic, with the strongest scattering occurring in the direction of SPP incidence and with the anisotropy decreasing with the increase of the particle-surface distance. The differential cross section for the SPP scattering into the waves propagating away from the surface has been found to exhibit similar angular behavior for relatively small particle-surface distances. The total cross sections for these scattering channels have been compared for different values of the metal dielectric constant. In general, the results obtained were found in good agreement with the results of previous theoretical considerations in Refs. 23 and 31. Finally, verification of the energy conservation in the scattering process allowed us to establish the conditions for the validity of the point-dipole approach for the SPP scattering by a small spherical particle. We have obtained the additional requirements imposed on the system parameters that have been further simplified for two practical configurations. We believe that the results obtained can be used in order to justify the usage of the (relatively simple) point-dipole approximation, perhaps even in the scalar form, for modeling of various SPP scattering phenomena, e.g., occurring in SPP micro-optical elements. It should be borne in mind, however, that our consideration concerns an individual particle illuminated by a plane SPP and that the situation with closely placed (or even touching) particles is quite different, because the field incident on a particle can no longer be considered constant across the particle. Still, if the interparticle distance is sufficiently larger than the particle size, one can neglect the latter effect and make use of the results obtained in our paper.

*Electronic address: a.b.evlyukhin@mail.ru

[1] *Surface Polaritons*, edited by V. M. Agranovich and D. L. Mills (North-Holland, Amsterdam, 1982); H. Raether, *Surface Plasmon*, Vol. III of Springer Tracts in Modern Physics (Springer, Berlin, 1988).
[2] W. L. Barnes, A. Dereux, and T. W. Ebbesen, Nature (London) **424**, 824 (2003).
[3] F. Pincemin, A. A. Maradudin, A. D. Boardman, and J.-J. Greffet, Phys. Rev. B **50**, 15 261 (1994).
[4] J. A. Sanchez-Gil, Phys. Rev. B **53**, 10 317 (1996).
[5] J. A. Sanchez-Gil and A. A. Maradudin, Phys. Rev. B **60**, 8359 (1999).
[6] U. Schröter and D. Heitmann, Phys. Rev. B **58**, 15 419 (1998).
[7] J. A. Sanchez-Gil and A. A. Maradudin, Opt. Express **12**, 883 (2004).
[8] A. Bouhelier, T. Huser, H. Tamaru, H.-J. Güntherodt, D. W. Pohl, F. I. Baida, and D. Van Labeke, Phys. Rev. B **63**, 155404 (2001).
[9] J. R. Krenn, M. Salerno, N. Felidj, B. Lamprecht, G. Schider, A. Leitner, F. R. Aussenegg, J.-C. Weeber, A. Dereux, and J. P. Goudonnet, J. Microsc. **202**, 122 (2001).
[10] J.-C. Weeber, J. R. Krenn, A. Dereux, B. Lamprecht, Y. Lacroute, and J. P. Goudonnet, Phys. Rev. B **64**, 045411 (2001).
[11] S. I. Bozhevolnyi and F. A. Pudonin, Phys. Rev. Lett. **78**, 2823 (1997).
[12] I. I. Smolyaninov, D. L. Mazzoni, J. Mait, and C. C. Davis, Phys. Rev. B **56**, 1601 (1997).
[13] H. Ditlbacher, J. R. Krenn, G. Schider, A. Leitner, and F. R. Aussenegg, Appl. Phys. Lett. **81**, 1762 (2002).
[14] J. Saxler, J. Gomez Rivas, C. Janke, H. P. M. Pellemans, P. Haring Bolivar, and H. Kurz, Phys. Rev. B **69**, 155427 (2004).
[15] S. Bozhevolnyi and V. Volkov, Opt. Commun. **198**, 241 (2001).
[16] T. Søndergaard and S. I. Bozhevolnyi, Phys. Rev. B **67**, 165405 (2003).
[17] S. I. Bozhevolnyi, J. Erland, K. Leosson, P. M. W. Skovgaard, and J. M. Hvam, Phys. Rev. Lett. **86**, 3008 (2001).
[18] S. I. Bozhevolnyi, V. S. Volkov, K. Leosson, and A. Boltasseva, Appl. Phys. Lett. **79**, 1076 (2001).
[19] V. S. Volkov, S. I. Bozhevolnyi, K. Leosson, and A. Boltasseva, J. Microsc. **210**, 324 (2003).
[20] M. Kretschmann and A. A. Maradudin, Phys. Rev. B **66**, 245408 (2002).
[21] M. Kretschmann, Phys. Rev. B **68**, 125419 (2003).
[22] J. Joannopoulos, J. Winn, and R. Meade, *Photonic Crystals: Molding the Flow of Light* (Princeton University Press, Princeton, NJ, 1995).
[23] A. V. Shchegrov, I. V. Novikov, and A. A. Maradudin, Phys. Rev. Lett. **78**, 4269 (1997).
[24] S. I. Bozhevolnyi and V. Coello, Phys. Rev. B **58**, 10 899 (1998).
[25] V. Coello, T. Søndergaard, and S. I. Bozhevolnyi, Opt. Commun. **240**, 345 (2004).
[26] C. Girard and A. Dereux, Phys. Rev. B **49**, 11 344 (1994).
[27] L. Novotny, B. Hecht, and D. Pohl, J. Appl. Phys. **81**, 1798 (1997).
[28] C. Beitia, Y. Borensztein, R. Lazzari, J. Nieto, and R. G. Barrera, Phys. Rev. B **60**, 6018 (1999).
[29] P. C. Chaumet, A. Rahmani, F. de Fornel, and J.-P. Dufour, Phys. Rev. B **58**, 2310 (1998).
[30] M. Quinten, A. Pack, and R. Wannemacher, Appl. Phys. B: Lasers Opt. **68**, 87 (1999).
[31] T. Søndergaard and S. I. Bozhevolnyi, Phys. Rev. B **69**, 045422 (2004).
[32] O. Keller, M. Xiao, and S. Bozhevolnyi, Surf. Sci. **280**, 217 (1993).
[33] M. Xiao, S. Bozhevolnyi, and O. Keller, Appl. Phys. A: Mater. Sci. Process. **62**, 115 (1996).
[34] A. B. Evlyukhin and E. V. Evlyukhina, J. Opt. Technol. **71**, 384 (2004).
[35] P. Gay-Balmaz and O. Martin, Opt. Commun. **184**, 37 (2000).
[36] Z. Li, B. Gu, and G. Yang, Phys. Rev. B **55**, 10 883 (1997).
[37] L. Novotny, J. Opt. Soc. Am. A **14**, 105 (1997).
[38] E. Palik, *Handbook of Optical Constant of Solids* (Academic, San Diego, CA, 1985).
[39] M. Born and E. Wolf, *Principles of Optics* (Pergamon, Oxford, 1970).
[40] J. D. Jackson, *Classical Electrodynamics* (Wiley, New York, 1975).
[41] B. T. Draine, Astrophys. J. **333**, 848 (1988).
[42] M. A. Taubenblatt and T. K. Tran, J. Opt. Soc. Am. A **10**, 912 (1993).
[43] O. Keller, Phys. Rep. **268**, 85 (1996).